JST: Smart Systems and Devices
Volume 33, Issue 3, September 2023, 008-015

Multi-Band Antenna Design Optimization Using Nature-Inspired Evolutionary Algorithm for 5G Wireless Communication

Nguyen Duc Hai, Nguyen Thanh Huong, Le Minh Hoang*
School of Electrical and Electronic Engineering, Hanoi University of Science and Technology, Ha Noi, Vietnam
**Corresponding author email: hoang.leminh@hust.edu.vn*

Abstract

Automation and telecommunication systems are increasingly improving and becoming more easily integrated thanks to wireless communication technology, in which the essential component is the antenna. Designing and optimizing antenna structures still takes a lot of time, especially for complex structures with multiple operating frequency bands or complex material layers. With modern computing power, the speed of computation is increasingly efficient, and combining automated computation for optimization and design is entirely feasible. Many research groups around the world have implemented automated antenna design through optimization algorithms, genetic algorithms, swarm algorithms, collectively referred to as evolutionary algorithms. These algorithms simplify the antenna design process, making it more automated and optimized. In this paper, the Improved Black Hole algorithm is proposed and used to optimize the design of a CPW-Fed slot microstrip antenna.

Keywords: Nature-inspired optimization, Black Hole algorithm, antenna design, 5G communication, multi-band antenna, Sub-6 GHz band

1. Introduction

The development of information and communication technologies with an increasing number of users and the demand for high flow rates has led to in-depth research on fifth-generation (5G) mobile communications. Technologies for the 5G systems have been studied to determine and standardize telecommunication protocols, modulation, bandwidth, and communication frequencies, as well as to design antennas and antenna systems that support the requirements of the 5G system. With well-defined criteria, the systems which operate on multiple frequencies need to be augmented. Therefore, applying algorithms to optimize antenna designs is crucial.

Optimization is necessary in all engineering fields to address diverse issues. Optimization methods with high-intensity computations become more useful as the scale of the problem increases. This is highly relevant to antenna design requirements, and algorithms inspired by natural processes have been applied to antenna design optimization, including the genetic algorithm (GA) [1, 2], particle swarm optimization (PSO) [3, 4], and their variants [5, 6]. In this paper, an algorithm based on the Black Hole (BH) phenomenon and a Multiband Coplanar-Fed Microstrip Antenna is proposed.

In this paper, a typical representation of the nature-inspired evolved antenna is investigated and developed. The Black Hole (BH), a space-operated phenomenon, is used as an evolutionary algorithm to optimize the antenna structure. The concept of the Black Hole algorithm (BHA) is described in Section 2 with the modified mechanism applied for antenna design optimization. The multiband antenna structure is introduced and calculated in Section 3. Finally, the algorithm as well as antenna structure are verified by simulation and then validated by measurement results.

2. Black Hole Algorithm

2.1. Introduction

The Black Hole algorithm was first introduced by Abdolreza Hatamlou in 2013 [7]. This algorithm is inspired by the phenomenon of black holes (BHs). In the real world, a BH is an object with an extremely high density and a strong gravitational force. The gravitational force of a BH devours any object that comes close enough. This algorithm and its variants have been used to solve many technical, medical, biological, and optimization problems, such as the multi-objective reactive power dispatch problem [8], optimal coordination of digital overcurrent relays problem [9], feature selection and classification on biological data [10] and optimizing extreme learning machine soft-sensor model [11].

BHA is a new population-based optimization algorithm that serves as a novel mechanism for Particle Swarm Optimization (PSO). In BHA, stars play the role of the population, and the best individual is chosen

ISSN: 2734-9373
https://doi.org/10.51316/jst.168.ssad.2023.33.3.2
Received: June 27, 2023; accepted: August 1, 2023

as the BH, which starts absorbing the surrounding population. The movement process of BHA involves the motion of stars by updating their positions to a new location closer to the BH, as follows:

$$X_{n,new} = X_n + rand(.)(Best^k - X_n); \quad n = 1, \dots, NL \tag{1}$$

where X_n and $X_{n,new}$ are the respective position of the target and updated agent n. NL is the number of learners in the population. $rand(.)$ is the random generator function in the range [0,1]. $Best^k$ is the position of the best solution in each iteration k. During the movement process of each candidate's solution toward the BH $Best^k$, there is a probability of crossing the event horizon.

A shape like a sphere exists around the BH called the event horizon and its radius is called Schwarzschild radius which can be calculated by using (2):

$$R = \frac{f_{BH}}{\sum_{i=1}^{N} f_i} \tag{2}$$

where f_i and f_{BH} are the fitness values of the BH and its star. N is the number of stars (candidate solutions).

2.2. Improved Black Hole Algorithm

Due to the characteristics of BHs, the Black Hole algorithm (BHA) has many advantages, such as powerful optimization, simple structure, easy implementation, few parameters, and fast convergence. However, on the other hand, it also has some disadvantages that make it unable to solve complex and high-dimensional problems. The main problem of BHA is that it cannot find a good balance between exploration and exploitation. It focuses more on the areas around the selected black hole, making it easy to get trapped in local optima. Furthermore, stars always follow a single path toward the best solution, which limits the algorithm's exploration ability.

To cope with these limitations, an improved version of the Black Hole algorithm has been proposed. The combination of the Black Hole algorithm and mutation and crossover operators inspired by the GA algorithm has created the Improved Black Hole (IBH) algorithm [12, 13]. This combination allows the IBH algorithm to explore the space around the black hole better and achieve good results with fewer iterations.

2.3. Stars Absorption

During the progress of the algorithm, the stars progressively move closer to the black hole, and if any star crosses the event horizon, it gets swallowed by the black hole, resulting in its removal from the current population. A new star is regenerated in the search space using an appropriate method, and eventually, it is reintroduced into the current population. Whenever a star is swallowed by the BH, a new star is created using one of the following strategies:

1. Randomly generate a new star with a probability of 0.7 (using a uniform distribution).
2. Create a new star by randomly selecting two stars from the population and combining their attributes through a combination method using the GA algorithm. The best star resulting from the recombination process is then added to the population. The method is applied with a probability of 0.3.

2.4. Pseudo Code for IBH Algorithm

```
Input
Number of starts (N), number of iteration
Output
Black hole
The fitness value of black hole
Begin
Initialize a population of stars randomly
For j = 1 to numbers of stars
        Evaluate the fitness value of star
The star with the most remarkable fitness
value is chosen as the black hole
While (max iteration or convergence criteria is
not met) do
    For each star in the current population:
        Move the star toward the black hole
        Evaluate fitness value of the star
        Set the star as a black hole if it's better
than the current black hole
    End for
    Calculate the radius of the event horizon for
the new selected black hole
    If round(iteration/max_iteration,1) * 10% 2
== 0
        Evolution_rate = 0.7
    Else
        Evolution_rate = 0.3
    End if
    For each star in the current population:
        If the distance between the star and the
black hole is less than the event horizon radius
        Remove the star from the population
        If random() <= Evolution_rate
            Split the current population into two
equal sets (male and female sets)
            Select two stars randomly, one from
each set.
            Perform two split point crossover
between the selected stars.
            Select the better of the two generated
stars to be the new star.
```

```
        Else
            Generate new star randomly
        End if
        Add the generated star to the
    population.
        End if
        Set the star as a black hole of it's better
    than the current black hole.
    End for
    End while
Return the current black hole.
```

3. Proposed Antenna

The use of coplanar waveguide in multi-band antennas as antenna feed is important so that the antenna will be compatible with monolithic microwave integrated circuits. Coplanar waveguide has several advantages such as easy integration with active and passive elements, low frequency dispersion, the extra design freedom through the ability to vary the characteristic impedance and phase constant by changing the slot and strip widths, and avoiding the excessively thin, and therefore fragile, substrates as in microstrip line [14, 15].

The design of CPW antennas for 5G has recently attracted much attention. Wei Hu *et al* [16], designed a dual-band eight-element MIMO array using multi-slot decoupling technique for 5G terminals with multiple Printed Circuit Boards (PCBs). Abed and Jawad [17] proposed a compact size MIMO fractal slot antenna for 3G, LTE (4G), WLAN, WiMAX, ISM and 5G communications using CPW feed.

Some candidate bands have been investigated and used as 5G band in Vietnam, for example, 2.5 - 2.6 GHz, 3.7 - 3.8 GHz, 6.4 - 7.1 GHz. In this paper, we propose a novel compact tri-band patch antenna fed by a coplanar waveguide (CPW) line for 2.55 GHz, 3.75 GHz, and 6.6 GHz.

The geometry and parameters of the proposed antenna fed by a CPW line are shown in Fig. 1. The patch antenna is printed on a dielectric substrate of a height equal to 1.6 mm and a relative permittivity of 4.4. The width of the 50 Ω microstrip fed line is 2.74 mm.

The parameters and the variation intervals of the parameters for the antenna are listed in Table 1.

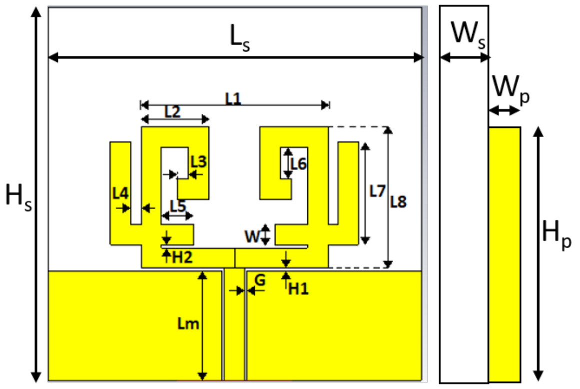

(a) (b)

Fig. 1. The proposed antenna structure: a) Front view, b) Side view.

Table 1. Geometrical parameters of the antenna

Parameter	L_S	H_S	W_S	W_p	H_p	W
Value (mm)	40	40	1.6	0.035	35	2.74
Parameter	G	H1	H2	L1	L2	L3
Value (mm)	0.27	0.35	0.4	25	[6.8, 12.28]	[0, L2]
Parameter	L4	L5	L6	L7	L8	Lm
Value (mm)	[0.2, 3.0]	[1.0, 9.76]	[2.0, 7.5]	[4.74, 15.86]	19	16

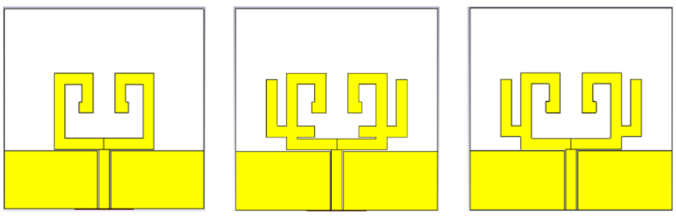

(a) (b) (c)

Fig. 2. Development of proposed CPW fed triband antenna geometry; (a) single band 2.55GHz (b) 2.55GHz, 3.75GHz and (c) triband 2.55GHz, 3.75Ghz and 6.6GHz.

In order to make the proposed antenna, we have to place the different branches for the antenna to investigate the development of antenna and integrate different frequency bands. The development is proposed in Fig. 2.

The CPW-fed triband antenna geometry reported here is developed from the single band microstrip antenna in Fig. 2(a). The structure is converted into a dual band antenna with resonances at 2.55 GHz and 3.75 GHz by introducing two "L" shaped slots as shown in Fig. 2(b). Another slot is introduced in Fig. 2(c) to produce the third resonance around 6.6 GHz. The dimensions of the antenna development are based on Fig. 1 and Table 1. To obtain the design for the length of different branches, the reflection coefficient needed to be calculated and simulated. Fig. 3 exhibits the results after design and simulation for each step to make the whole antenna.

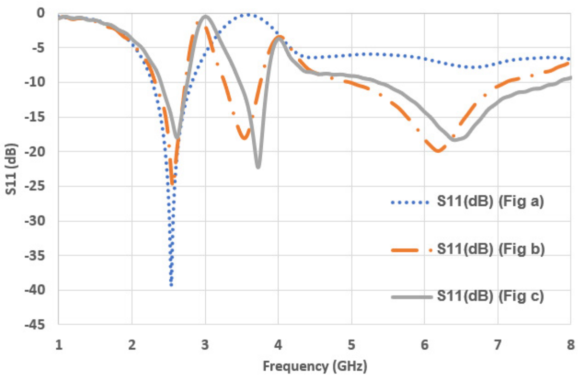

Fig. 3. Reflection coefficients of single band, dual band and triband antenna geometries shown in Fig. 2 (a) to (c).

The parameters for optimal antenna design which are selected to achieve the compact dimension and possibly good features such as high radiation efficiency, etc., are presented in the next section. The antenna was simulated, and its prototype was fabricated and then measured.

4. Optimizing Antennas by the Improved Black Hole Algorithm (IBH)

The aim of this part is to minimize the average value of the S11 module (in dB) in the three bands of 5G ([2.5 2.6] GHz, [3.7 3.8] GHz, [6.4 7.1] GHz)

In this case, the multi-objective optimization function of the reflection coefficient must meet the following requirements:

$S_{11} \leq -10$ dB for 2.55 GHz, 3.75 GHz and 6.6 GHz

The block diagram of the IBH optimizer for antenna has been presented in Fig. 4.

The optimization procedure in this design has been summarized below:

Step 1: The first generation of individuals was randomly generated to provide the starting point for the optimization process. Each individual was modeled in CST for computation of the return losses S11 over the ranges of each frequency band. The fittest individuals were selected for BH and calculating the Schwarzschild radius of a BH.

Step 2: Update the position of individual stars approaching the BH position. Remove the star instances if the distance to the BH is less than the Schwarzschild radius and create a new one in one of two ways: Randomly generate or combine with GA algorithm. Fitness values of the offspring were computed.

Step 3: Select a new BH and recalculate the Schwarzschild radius.

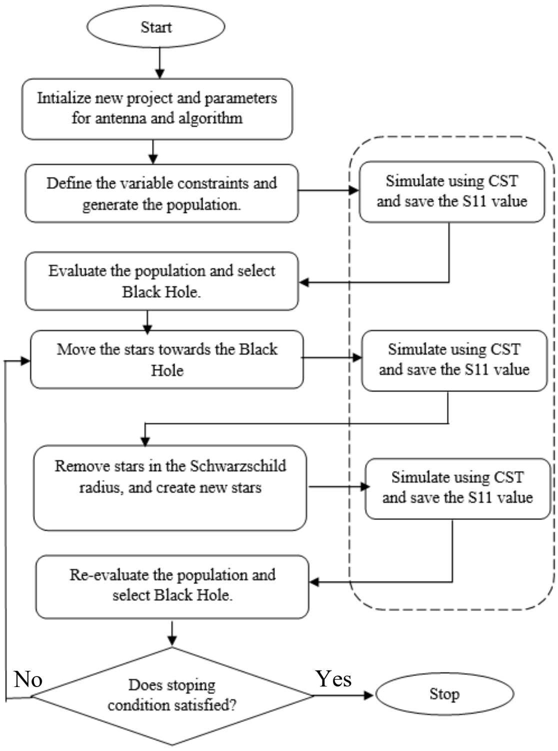

Fig. 4. The flowchart of IBH Algorithm.

Steps 2 and 3 are repeated until the criterion ends are met. In the process of optimizing IBH, the number of population members plays a crucial role and remains constant throughout the optimization process of the algorithm. A larger population size can potentially lead to better solutions. However, if the population size is excessively large, it will increase the computation time and reduce the algorithm's efficiency. Therefore, it is crucial to choose an appropriate population size which is parameterized in Fig. 5.

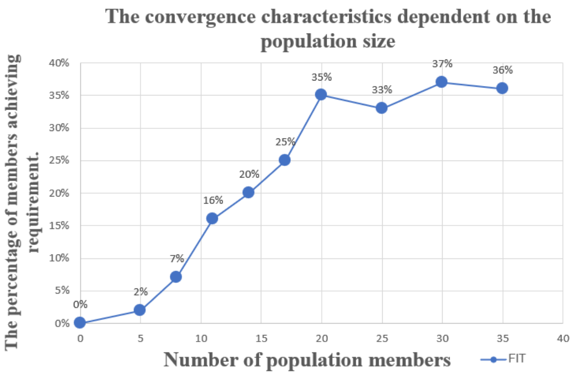

Fig. 5. The chart of the convergence characteristics with generations (GEN=15).

Based on Fig. 5, it can be observed that if the number of population members is too small, the convergence capability of the algorithm is significantly poor and tends to improve as the number of individuals increases. However, once the number of population members reaches a value approximately 3 to 6 times the optimal parameter, the convergence capability remains relatively stable. Therefore, it is advisable to choose the number of population members within the range of 3 to 6 times the optimal parameter.

In this paper, we constructed an optimization algorithm with six parameters: L_2, L_3, L_4, L_5, L_6 and L_7. And the IBH used optimization process has the following properties:

- Number of population members: 20,

- Number of generations: 16,

Table 2. The values of the reflection coefficient S_{11} for the BH optimization process for each generation

Generation	2.55Ghz	3.75Ghz	6.6GHz
1-S_{11} (dB)	-4.81	-9.73	-16.26
2-S_{11} (dB)	-4.97	-9.91	-16.48
3-S_{11} (dB)	-4.84	-10.35	-17.17
4-S_{11} (dB)	-4.91	-10.85	-15.31
5-S_{11} (dB)	-7.78	-13.73	-13.19
6-S_{11} (dB)	-15.39	-8.51	-15.90
7-S_{11} (dB)	-17.58	-9.13	-14.35
8-S_{11} (dB)	-16.89	-9.47	-14.58
9-S_{11} (dB)	-18.99	-10.55	-13.61
10-S_{11} (dB)	-19.02	-11.85	-10.94
11-S_{11} (dB)	-14.21	-12.97	-12.51
12-S_{11} (dB)	-15.70	-17.65	-15.14
13-S_{11} (dB)	-15.55	-19.19	-16.23
14-S_{11} (dB)	-16.050	-21.690	-17.02
15-S_{11} (dB)	-16.059	-21.687	-17.00
16-S_{11} (dB)	-16.059	-21.691	-17.01

From the initial population of stars, stars are gradually replaced and progress towards BHs after each generation. After 16 generations, the fittest individual (BH) of each generation has a value of S11 according to Table 2.

The results obtained by a GA optimization are illustrated in Table 3. The final optimized antenna results will be presented in the next section.

Table 3. Optimized dimensions of the antenna

Parameters	Optimized value (mm)
L2	9.03
L3	1.453
L4	1.336
L5	4.346
L6	4.34
L7	13.8

5. Result and Discussions

The optimized antenna with size of 40x40 mm^2 and simulated antenna (using commercial software, namely CST MWS) is shown in Fig. 6.

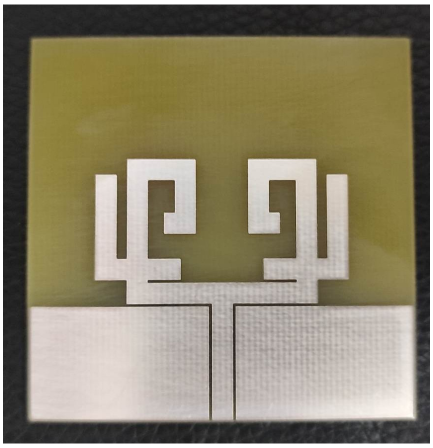

Fig. 6. Photograph of optimized antenna

The performance parameters deduced here are re-reflection coefficient, surface current distribution, and far-field characteristics, gain, efficiency and radiation patterns.

5.1. Reflection Coefficient

The reflection coefficient versus frequency of the proposed antenna is shown in Fig. 7. Fig. 7 shows the presence of three diverse resonant frequencies which are 2.55 GHz, 3.75 GHz, and 6.6 GHz, in which a good matching is satisfied.

These results show three diverse resonant frequencies with a small shift toward high frequencies. The small deviations between the simulated and measured results may be caused by the usual connectors and manufacturing errors. Moreover, the limitation of the EM simulator may lead to discrepancies between the simulated and measured results. Usually, such discrepancies may be attributed to the dielectric material that should be characterized before realization since its properties deviate from those set in the software simulator.

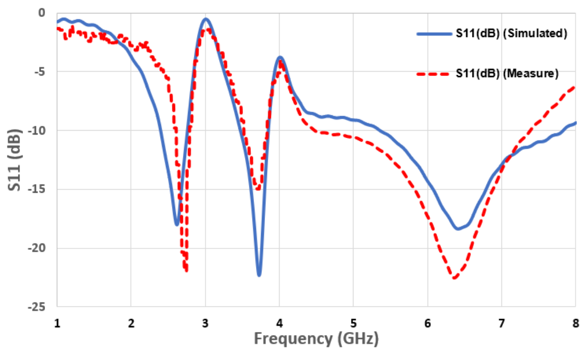

Fig. 7. The input reflection coefficient versus frequency.

5.2. Surface Current Distribution

In order to further investigate the return loss performance of the proposed antenna, the surface current distribution plots at its three bands 2.55 GHz, 3.75 GHz, and 6.6 GHz are depicted in Fig. 8(a) to (c) using CST. At 2.55 GHz, the current is mainly concentrated along the horizontal stub and its flared element. Resonance at 3.75 GHz is influenced by “L” shaped slots. The role of the slot in the horizontal stub is evidenced with the surface current distribution along its edges in Fig. 8(c). It is shown through the resonant frequency of 6.6 GHz.

5.3. Far-Field Antenna Performance

The simulated far-field radiation patterns of the proposed antenna at three resonance frequencies are plotted in Fig. 9. The realized gains are obtained with values of 2.085 dBi, 3.474 dBi and 3.907 dBi at frequencies of 2.55 GHz, 3.75 GHz, and 6.6 GHz respectively. It seems that at high frequencies, the antenna radiates more directively and achieves better gain and efficiency.

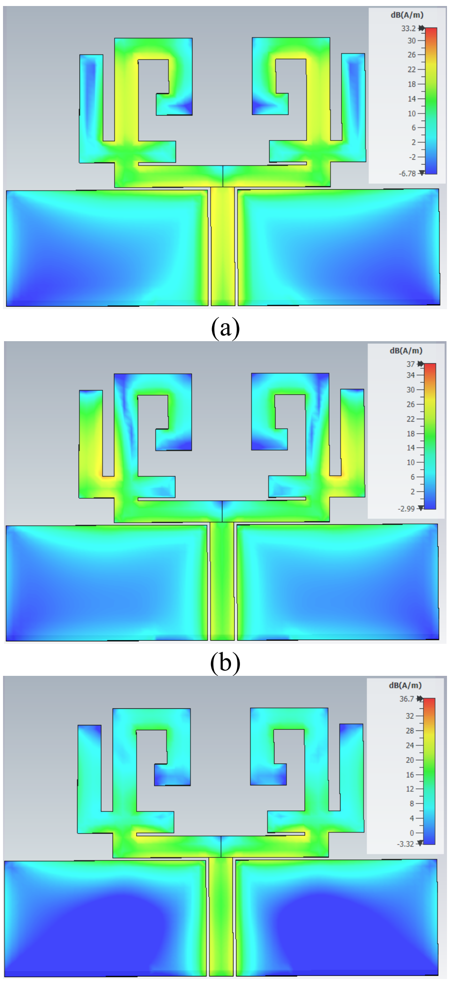

(a) (b) (c)

Fig. 8. Current distribution at three distinct frequencies: (a) f = 2.55 GHz, (b) f = 3.75 GHz, and (c) f = 6.6 GHz.

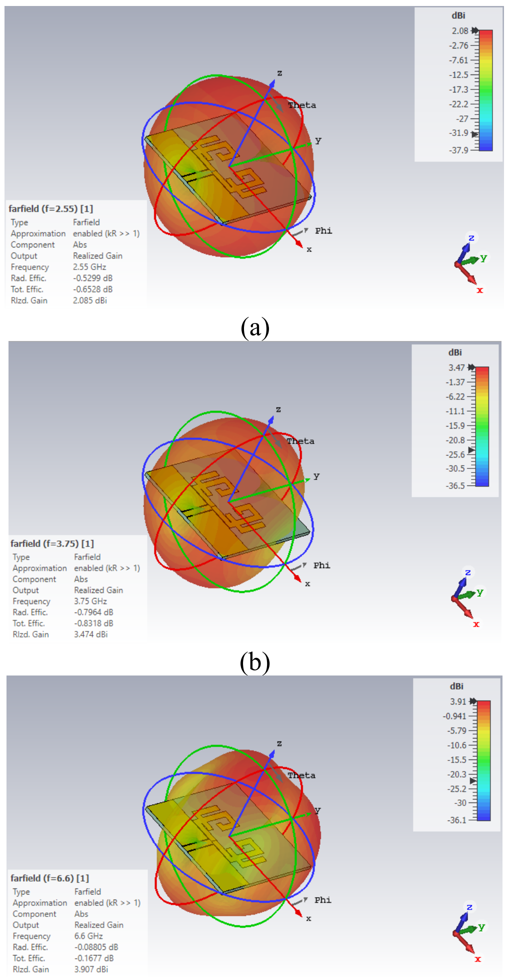

(a) (b) (c)

Fig. 9. 3-D Radiation Patterns and Realized Gain at three distinct frequencies: (a) f = 2.55 GHz, (b) f = 3.75 GHz, and (c) f = 6.6 GHz.

Meanwhile, Fig. 10 shows the 2D radiation patterns at three distinct frequencies in the plans: (a) θ = 90°, (b) φ = 90°, and (c) φ = 0°. In the E-plane (φ = 90°) and H-plane (φ = 0°), Fig. 10 (b and c), the radiation pattern is bidirectional oriented towards the angles θ = 0° and θ = 180° for the three resonant frequencies. Consequently, the proposed antenna pattern looks like that of a dipole.

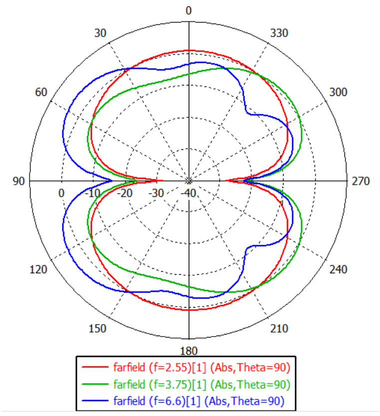

(a)

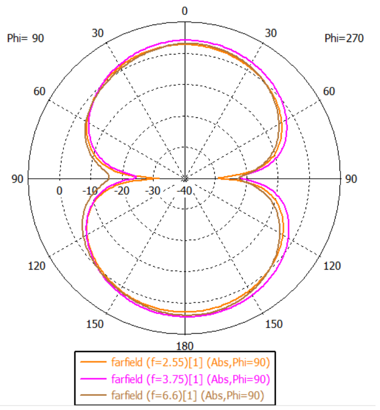

(b)

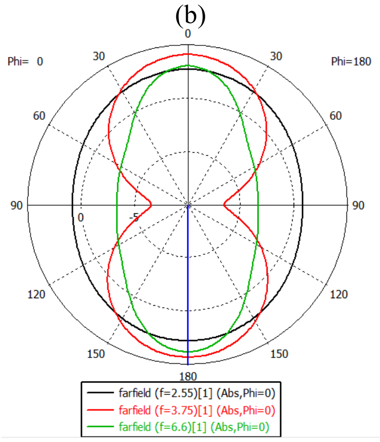

(c)

Fig. 10. 2-D radiation patterns at three distinct frequencies in the planes: (a) θ = 90°, (b) φ = 90°, and (c) φ = 0°.

The multiband antennas nowadays attract more attention. Various groups have carried out their research on multiband antenna, from dual bands to quad bands. In Table 4, we made a comparison with recent research on multiband antennas. Our antenna performs a better dimension and gain as compared with the other researched antennas which have triple band design. With the assistance of the evolutionary algorithm and the resource of hardware (CPU quadcore 3.2 GHz and 32 GB RAM), the automated antenna design for sub-6GHz 5G communication becomes more feasible than ever.

Table 4. Comparison with other triple band antennas

Antenna type	Frequency bands	Gain/ Realized gain	Dimension
4-element MIMO antenna [18]	3.77 GHz 4.71 GHz 6.31 GHz	2.5 dBi 3.26 dBi 3.3 dBi	160mm x 160 mm
Ground-Coupled CPWG-Fed MIMO antenna [19]	5.5 GHz 5.85 GHz 7.125 GHz	3.5 dBi - 3.9 dBi	40 mm x 40 mm
Dual-Polarized Dipole antenna [20]	3.6-3.85 GHz 4.05-4.2 GHz 4.8-5.15 GHz	8 dBi - 9 dBi	120 mm x 120 mm
Our proposed antenna	2.55 GHz 3.75 GHz 6.6 GHz	2.085 dBi 3.474 dBi 3.907 dBi	40 mm x 40 mm

6. Conclusion

This paper presented the application of an Improved Black Hole algorithm for optimizing the novel compact tri-band antenna fed by a CPW line. The proposed antenna with IBH optimization provided triple-band operation at [2.5-2.6] GHz, [3.7-3.8] GHz, [6.4-7.1] GHz. At the centre frequencies 2.55, 3.75, and 6.6 GHz, the peak gains were 2.25, 3.52, and 3.981 dBi, correspondingly. With these qualities, the proposed antenna can be used for 5G applications in Vietnam. For future study, IBH algorithms can be applied to optimize multi-band microstrip antenna for maximum gains and minimum return losses at desired frequencies. Furthermore, for enhanced bandwidth, wideband feeding techniques should be employed.

Acknowledgments

This research is funded by Hanoi University of Science and Technology (HUST) under grant number T2021-PC-022.

References

[1] A. H. Hussein, H. H. Abdullah, A. M. Salem, S. Khamis, and M. Nasr, Optimum design of linear antenna arrays using a hybrid MoM/GA algorithm, IEEE Antennas and Wireless Propagation Letters, vol. 1, pp. 1232-1235, October 2011. https://doi.org/10.1109/LAWP.2011.2174189

[2] D. Zhou, R. A. Abd-Alhameed, C. H. See M. S. Bin-Melha, etc., New antenna designs for wideband harmonic-suppression using adaptive surface meshing and genetic algorithms", IET Microwaves, Antennas & Propagation, 2011, pp.1054 - 1061. https://doi.org/10.1049/iet-map.2010.0218

[3] J. Robinson, and Y. Rahmat-Samii, Particle swarm optimization in electromagnetics, IEEE Transactions on Antennas and Propagation, vol.52, pp. 397-407, 2004. https://doi.org/10.1109/TAP.2004.823969

[4] H. J. Mohammed, A. S. Abdullah, R. S. Ali, R. A. Abd-Alhameed, Y. I. Abdulraheem, & J. M. Noras, "The design of a uniplanar printed triple band rejected uwb antenna using particle swarm optimization and the firefly algorithm", IET MAP, vol. 11, issue 1, 2016, pp. 31-37. https://doi.org/10.1049/iet-map.2014.0736

[5] J. M. Johnson and Y. R. Samii, Genetic algorithms in engineering electromagnetics, IEEE Antennas Propagation Magazine, vol. 39, no. 4, pp. 7-21, 1997. https://doi.org/10.1109/74.632992

[6] M. A. Panduro and C. A. Brizuela, A comparative analysis of the performance of GA, PSO and DE for circular antenna arrays, in Proc. Antennas Propag. Soc. Int. Symp., 2009, pp. 1-4 https://doi.org/10.1109/APS.2009.5171514

[7] A. Hatamlou, Black hole: A new heuristic optimization approach for data clustering, Inf. Sci. 222 pp.175-184, 2013 https://doi.org/10.1016/j.ins.2012.08.023

[8] K. Lenin, B. R. Reddy, and M. S. Kalavathi, Black hole algorithm for solving optimal reactive power dispatch problem, International Journal of Research in Management, Science and Technology, vol. 2, pp. 2321-3264, 2014. https://doi.org/10.12720/ijeee.2.4.321-326

[9] N. Ghaffarzadeh and S. Heydari, Optimal coordination of digital overcurrent relays using black hole algorithm, TI Journals of World Applied Programming, vol. 5, pp. 50-55, 2015.

[10] E. Pashaei, N. Aydin, Binary black hole algorithm for feature selection and classification on biological data. Applied Soft Computing, vol. 56, pp. 94-106, 2017. https://doi.org/10.1016/j.asoc.2017.03.002

[11] W. Xie, J. S. Wang, C. Xing, S. S. Guo, M. W. Guo, L. F. Zhu, Extreme learning machine soft-sensor model with different activation functions on grinding process optimized by improved black hole algorithm. IEEE Access 8, pp. 25084- 25110, 2020. https://doi.org/10.1109/ACCESS.2020.2970429

[12] Yaghoobi, Saber, Mojallali, Hamed, Modified black hole algorithm with genetic operators, International Journal of Computational Intelligence Systems, vol 9 (4), pp. 652-665, 2016. https://doi.org/10.1080/18756891.2016.1204114

[13] H. Deeb, A. Sarangi, D. Mishra, S. K. Kumar Sarangi, Improved black hole optimization algorithm for data clustering, J King Saud Univ-Comput Inf Sci, vol. 34, pp. 5020-5029, 2022. https://doi.org/10.1016/j.jksuci.2020.12.013

[14] J. Chen, Dual-frequency slot antennas fed by capacitively coplanar waveguide, Microw. Opt. Technol. Lett., 32 (2002), pp. 452-453 https://doi.org/10.1002/mop.10207

[15] C. P. Wen, Coplanar waveguide: a surface strip transmission line suitable for nonreciprocal gyromagnetic device applications, IEEE Trans. Microw. Theor. Tech., 17 (1969), pp. 1087-1090 https://doi.org/10.1109/TMTT.1969.1127105

[16] W. Hu, Q. Long, S. Gao, Le-Hu Wen, L. Qi, H. Xu, X. Liu, W. Wang, Dual-band eight-element MIMO array using multi-slot decoupling technique for 5G terminals, IEEE Access, 7 (2019), pp. 153911-153920 https://doi.org/10.1109/ACCESS.2019.2948639

[17] A. T. Abed, A. M. Jawad, Compact size MIMO amer fractal slot antenna for 3G, LTE (4G), WLAN, WiMAX, ISM and 5G communications, IEEE Access, 7 (2019), pp. 125542-125551. https://doi.org/10.1109/ACCESS.2019.2938802

[18] Krishnamoorthy, R., Desai, A., Patel, R. et al. 4 Element compact triple band MIMO antenna for sub-6 GHz 5G wireless applications. Wireless Netw 27, 3747-3759 (2021). https://doi.org/10.1007/s11276-021-02734-8

[19] Kulkarni, J., Sim, CYD., Desai, A. et al. A Compact Four Port Ground-Coupled CPWG-Fed MIMO Antenna for Wireless Applications. Arab J Sci Eng 47, 14087-14103 (2022). https://doi.org/10.1007/s13369-022-06620-z

[20] Yang, L., Tahseen, H. U., Hussain, S. S. I. et al. Triple-band dual-polarized dipole antenna for 5G Sub-6 GHz Communications. Wireless Pers Commun 124, 2109-2120 (2022). https://doi.org/10.1007/s11277-021-09447-3